

Article

Assessment of Contact Pressures between a Mandibular Overdenture and the Prosthodontic Area

Małgorzata Idzior-Haufa ¹, Agnieszka A. Pilarska ^{2,*} , Tomasz Gajewski ³ , Krzysztof Szajek ³ , Łukasz Faściszewski ³, Piotr Boniecki ⁴, Krzysztof Pilarski ⁴, Magdalena Łukaszewska-Kuska ¹ and Barbara Dorocka-Bobkowska ¹ 

- ¹ Department of Gerodontology and Oral Pathology Chair of Prosthodontics, Poznan University of Medical Sciences, Bukowska Street 70, 60-812 Poznan, Poland; midziorhaufa@ump.edu.pl (M.I.-H.); mluk@ump.edu.pl (M.L.-K.); bdorocka@ump.edu.pl (B.D.-B.)
- ² Department of Plant-Derived Food Technology, Poznań University of Life Sciences, ul. Wojska Polskiego 31, 60-624 Poznan, Poland
- ³ Institute of Structural Analysis, Poznan University of Technology, Piotrowo 5 Street, 60-965 Poznan, Poland; tomasz.gajewski@put.poznan.pl (T.G.); krzysztof.szajek@put.poznan.pl (K.S.); lukasz.fasciszewski@put.poznan.pl (L.F.)
- ⁴ Department of Biosystems Engineering, Poznań University of Life Sciences, ul. Wojska Polskiego 50, 60-627 Poznan, Poland; bonie@up.poznan.pl (P.B.); pilarski@up.poznan.pl (K.P.)
- * Correspondence: pilarska@up.poznan.pl; Tel.: +48-61-848-73-08



Citation: Idzior-Haufa, M.; Pilarska, A.A.; Gajewski, T.; Szajek, K.; Faściszewski, L.; Boniecki, P.; Pilarski, K.; Łukaszewska-Kuska, M.; Dorocka-Bobkowska, B. Assessment of Contact Pressures between a Mandibular Overdenture and the Prosthodontic Area. *Appl. Sci.* **2021**, *11*, 4339. <https://doi.org/10.3390/app11104339>

Academic Editors: Bruno Chrcanovic and Luca Testarelli

Received: 26 March 2021

Accepted: 7 May 2021

Published: 11 May 2021

Publisher's Note: MDPI stays neutral with regard to jurisdictional claims in published maps and institutional affiliations.



Copyright: © 2021 by the authors. Licensee MDPI, Basel, Switzerland. This article is an open access article distributed under the terms and conditions of the Creative Commons Attribution (CC BY) license (<https://creativecommons.org/licenses/by/4.0/>).

Abstract: In this paper, we assess the pressure between the overdenture located in the mandible and supported by a bar retained on two implants and the prosthodontic area. For testing, a model of an edentulous mandible was created using a mold by FRASACO with two implants and a “rider” bar inserted. A complete mandibular denture with polypropylene matrices was made. Three types of matrices of various stiffness were applied. The mandible and overdenture geometry was mapped using a digital image obtained with a Steinbichler Comet L3D 3D scanner. Finite element method calculations were performed in the Abaqus FEA software. The results demonstrate that the maximum contact pressure is observed when the loads are associated with canines. A critical case for the lower posterior is chewing performed by the molars. The pressure zone is the largest for POM-1 with Young’s modulus of 1.5 GPa and is reduced by 5.0% and 7.8% for POM-2 (E = 2.5 GPa) and POM-3 (E = 3.5 GPa), respectively. The stress distribution under the prosthesis mostly depends on the region loaded onto it. The applied load produces a slight contact pressure between the denture and the prosthodontic area in the anterior zone. A change in polypropylene matrix stiffness does not affect contact pressures.

Keywords: bar; implant; contact pressure; matrix; mandible; finite element analysis

1. Introduction

Overdentures are used in rehabilitating the edentulous mandible. They are an economic compromise available to a wide range of patients [1,2]. Their relatively affordable price and simple clinical management, together with substantial improvements to retention and stability, make them an attractive and realistic treatment option, both for the patient and the dentist. However, the multitude of available types of overdentures [3–6] with respect to the number and locations of implants, as well as kinds of attachments (bars of various size, ball or “locator” attachments, telescopes), make a rational choice of the components difficult [7,8]. Despite the abundant literature, restoration design is often based on clinical tradition without considering theoretical foundations. Such negligence accompanied by performance failures or the lack of follow-up care may lead to unexpected and uncontrolled prosthesis rotation. The clinical implications of the above phenomena may not only include deviations in precision attachment mechanics and a change at the level of peri-implant tissues but may also lead to atrophy of the denture-bearing area

distally to the implants. According to Julius Wolff's law, atrophy is caused by excessive pressure on the prosthesis, referred to as "contact pressure" in the research terminology of mechanics [9]. In the method applied in this study, the authors use the above term to describe the areas of strain and relief in a model of the edentulous mandible restored with the overdenture supported by two implants and a bar. A situation was assumed where the edentulous maxilla was fitted with the complete denture.

In this paper, we assess the pressure between the overdenture located in the mandible supported by a bar retained on two implants and the prosthodontic area. Furthermore, the contact pressure distribution relative to the stiffness of polypropylene matrices was also studied.

2. Materials and Method

For testing, a model of an edentulous mandible was created using a mold (by FRASACO) with two implants inserted. The model was made of acrylic material (Probase Cold acrylic, Ivoclar Vivadent). The implants were placed parallel to each other in the area of the canines. Two-piece Osteopant Hex implants were applied, each 14 mm long and 4 mm in diameter [10,11]. These cylindrical-conical implants may be used for any bone, mainly in the procedure of delayed implantation. They have an asymmetrical thread with no sharp edges with a lead of 0.7 mm. This transfers strains onto the adjacent bone in an optimal manner. Their shape enables stable implant anchoring, even with a minimal amount of bony tissue. The implants are made of biocompatible titanium (cp Ti Grade IV); they are connected to prosthetic abutments with a hexagonal connection.

The next stage of the research process included preparing a prosthetic restoration. The selected material was a "rider" bar (PRECI-HORIX, CEKA). The bar was placed centrally in the alveolar part of the mandible, 1 mm above the top of the gingiva. The retentive element was cast using 4ALL metal. Finally, the prosthetic abutments were fixed in the surgical part of the implants using a screw made of a titanium-aluminum-vanadium alloy.

Next, a complete mandibular denture was fabricated (Figure 1). The prosthesis was made of Probase acrylic material. The artificial teeth (Wiedent) were positioned in a spherical plane. In its gingival surface, two symmetrically arranged matrix linings were embedded. Polypropylene matrices were placed in them. For the sake of the study, three types of matrices of various stiffness were applied (Young's modulus of 1.5, 2.5, and 3.5 GPa).



Figure 1. A model of an edentulous mandible with implants, a bar, and a complete denture.

2.1. Geometry Acquisition

A three-dimensional model of the cast (obtained in the previous research step) of the patient-specific mandible was created in a numerical environment for finite element method (FEM) input. The system consists of the following elements: the edentulous mandible, overdenture, and two splinted implants connected with the bar clip system (see Figure 2).

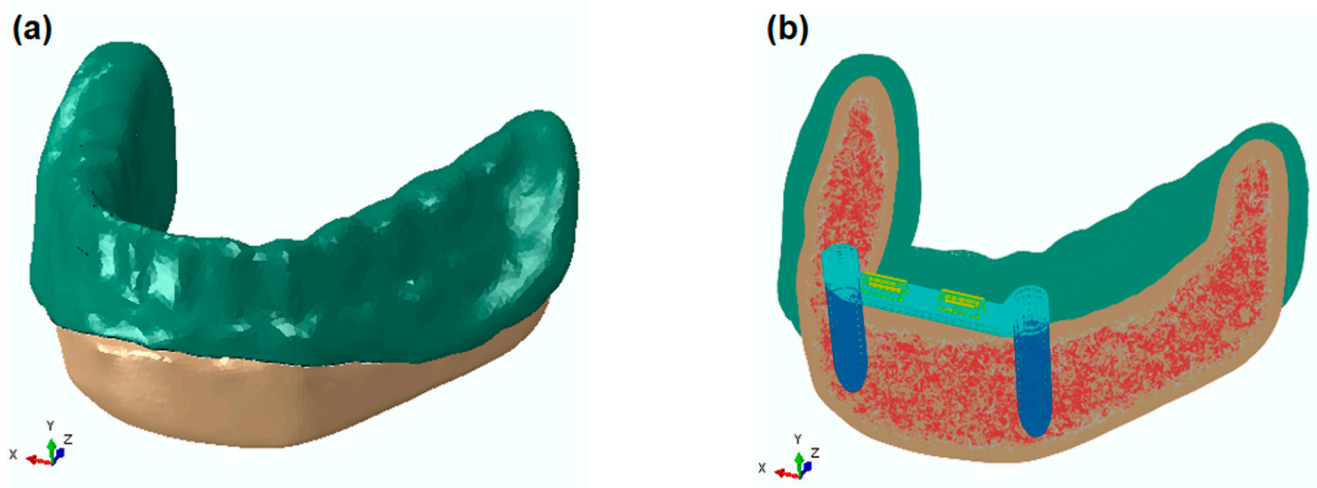


Figure 2. Numerical geometry of the system: (a) 3D view and (b) transparent 3D view.

The mandible and overdenture geometry were mapped using a digital image obtained with the Steinbichler Comet L3D 3D scanner. A stereolithographic image with 3296×2472 resolution was obtained, and the spatial distance between the neighboring points was $\sim 25\text{--}170 \mu\text{m}$, which ensured a very accurate description of the elements' surfaces (while the largest dimension of the mandible was a few centimeters). In the subsequent step, as a result of the preprocessing of data in STL format, the detailed surfaces of the elements were repaired (i.e., the surface holes were filled) and smoothed. Although the surface was smoothed, a graphic interpretation of the actual objects was obtained while maintaining the shape of the occlusal surface, the areas between teeth, and the nonregularities occurring on teeth crowns (Figure 3d).

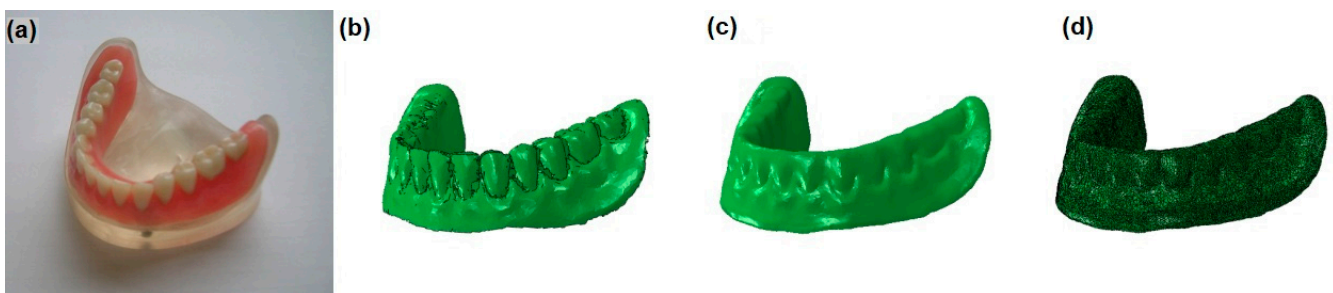


Figure 3. Steps of creating finite element mesh based on mandible cast: (a) input cast, (b) raw scanned data, (c) digitally processed model, (d) final finite element mesh.

In the edentulous mandible, three biological layers were separated: mucosa, cortical, and trabecular bone. The assumed cross section reflects the anatomical structure of the modeled system (Figure 4). Following the literature, the mucosa and the cortical bone were assumed to be 1.5 mm and 0.8 mm thick, respectively [12,13].



Figure 4. Cross-section of the mandible with assumed geometry of the layers.

The implants and bar clip system geometry were reproduced by computer-aided design software (CAD) based on the dimension measurements and product specification data (Osteoplast–Implant System; CEKA Attachments Preci-Line). In Figure 5, the geometry of the implant bar is presented.

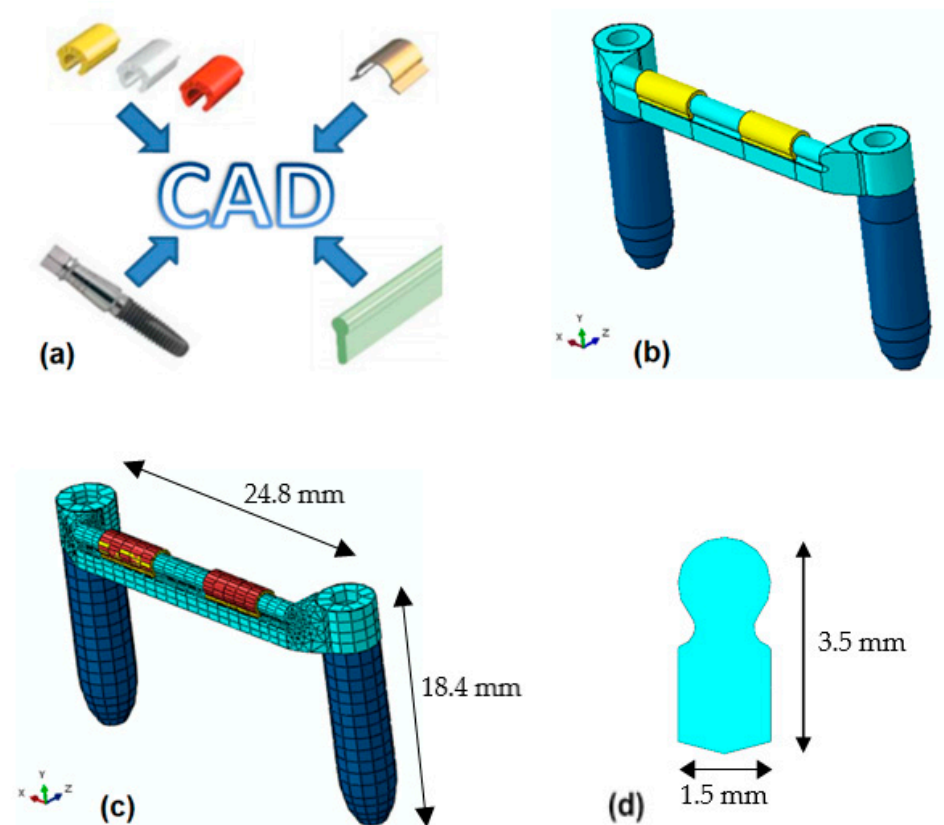


Figure 5. The geometry of the implant system: (a) assembly of clips, housing, bar, and implants; (b) computer-aided design model; (c) finite element mesh with main dimensions; and (d) bar cross section dimensions.

2.2. Finite Element Method Model

The particular parts described in the previous section were assembled in order to obtain the final finite element (FE) model of the overdenture prosthesis. Within the FE framework, linear 4-node elements [14] were assigned to the housing and linear 8-node brick elements [15] with reduced integration [16–19] to the prosthesis, bar, implants, clips, and edentulous mandible. The FE mesh was created to obtain a regular node pattern. The total number of model elements amounted to approximately 470 thousand, with the total number of the unknowns around 440 thousand.

In order to ensure realistic motion of the implant construction, a special FE technique was applied. Kinematic constraints were assigned to contact surfaces between the implants, bar, and clip matrices; thus, translational and rotational movements between the parts were excluded. No friction or material damping was assumed. A similar stiff connection (kinematic constraints) approach was used between the edentulous mandible and implant pillars; therefore, we considered the possible displacement between the implants and cortical bone (full implant–bone osteointegration) to be insignificantly small.

In order to avoid numerical difficulties due to mismatched FE meshes of the mandible and resin prosthesis, additional kinematic constraints were introduced, namely embedded elements [20]. The translational constraints provided (in physical meaning) well-fitted surfaces of the upper mandible and lower prosthesis and (in the mechanical sense) full compatibility of deformation fields.

A realistic condition of contact between the touching bodies was ensured. On the prosthesis mandible surface, the stiff (Herz-type) contact with no friction was defined [21,22]. Contact pressure depends on the normal forces between touching bodies; no influence of tangential forces is included. The separation of contact surfaces is possible due to a progressive deformation of bodies. The coefficient of tangential friction between the prosthesis and mucosa of the mandible is equal to zero under the assumption that saliva is present. Thus, the saliva lubrication gives an ideal slip between the surfaces, i.e., tangential pressures are equal to zero. There was no formal contact defined between the bone and the implant or the implant and the bar. The interactions between those bodies were modeled by tying them to the displacement (see Abaqus FEA documentation). Those connections were modeled as infinitely stiff.

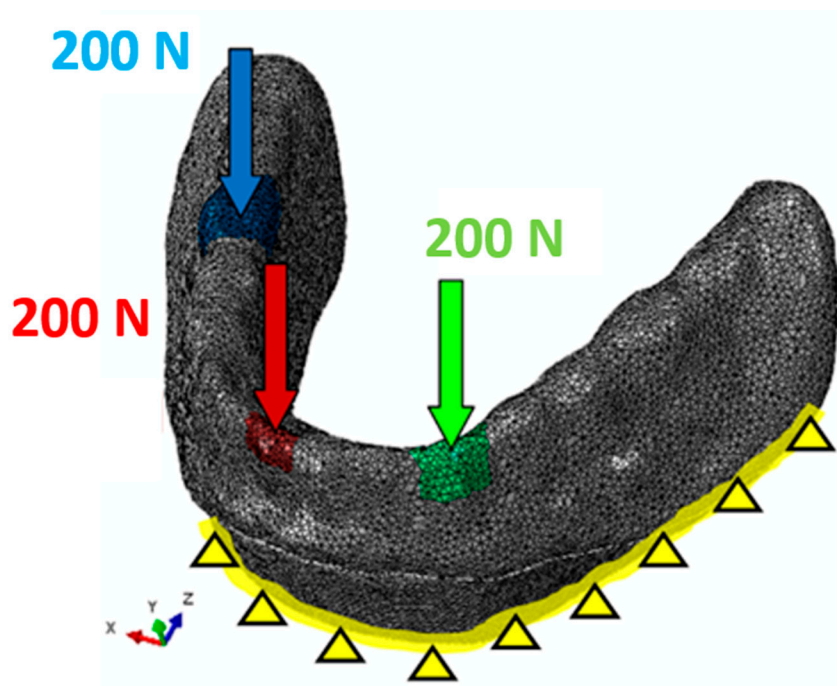
In this paper, classical isotropic linear elastic material models were used. Table 1 presents the adopted material parameters (the Young modulus, E ; and the Poisson's ratio, ν); the values were taken from the literature. In the research, the influence of stiffness on the bar clips was also investigated; therefore, three different Young moduli were used (1.5 GPa, 2.5 GPa, and 3.5 GPa) based on the commercially used materials.

The essential part of the numerical model description is the definition of the applied loads and the boundary conditions. Based on the literature and to obtain a realistic outcome of the modeled biomechanical system, we adopted a representative vertical force. The value of the force is equal to 200 N [29,30]. Three unsymmetrical positions of the occurrence of the force were chosen (three load cases). In each case, force is distributed on the surface of the particular tooth, mimicking occlusion pressure on a single tooth while eating. The canine, central incisor, and first molar were selected, according to Figure 6. The boundary conditions are an integral part of the FE model. In the presented paper, the nodes of the bottom surface of the edentulous mandible were restrained, as shown in Figure 6.

In the final part, finite element method calculations were performed in Abaqus FEA software (Dassault Systems). Nine linear stress analyses (three load cases, Figure 6, multiplied by three bar clip materials, see Table 1) were submitted. The purpose was to estimate the contact stress field between the resin prosthesis and the soft tissue of the mandible, as well as the influence of the clip stiffness on contact stresses. For each model, contact stresses, reduced (effective) stresses, and displacements were analyzed.

Table 1. Mechanical properties of the materials.

Materials (Parts)	Parameters		References
	Young Moduli (GPa)	Poisson's Ratio (-)	
acrylic resin (prosthesis)	2.8	0.28	[11]
Ti6Al4V (implants)	103.4	0.35	[11]
stainless steel (bar and implant pillar)	110.0	0.31	[10,23]
polypropylene (POM matrices)	1.5 2.5 3.5	0.45	[11,24,25]
INOX 316Ti (housing of the clips)	200.0	0.30	[26]
Mucosa (edentulous mandible)	0.001	0.45	[9,27,28]
cortical bone (edentulous mandible)	13.7	0.30	[11]
trabecular bone (edentulous mandible)	1.37	0.30	[11]

**Figure 6.** Finite element method model, three load cases, and boundary conditions.

3. Results and Discussion

The stress concentration in gingiva and nonuniform displacements of the overdenture are observed during loading. Maximal/minimal values are found near the mounting area of the implants and in the posterior zone (ramus mandibulae side), which indicates the point-like support (Figure 7). This also manifests itself in the movement of the prosthesis, which tends to cradle/swing on the dental beam and torsional modes, especially when posterior teeth are excited (Figure 8).

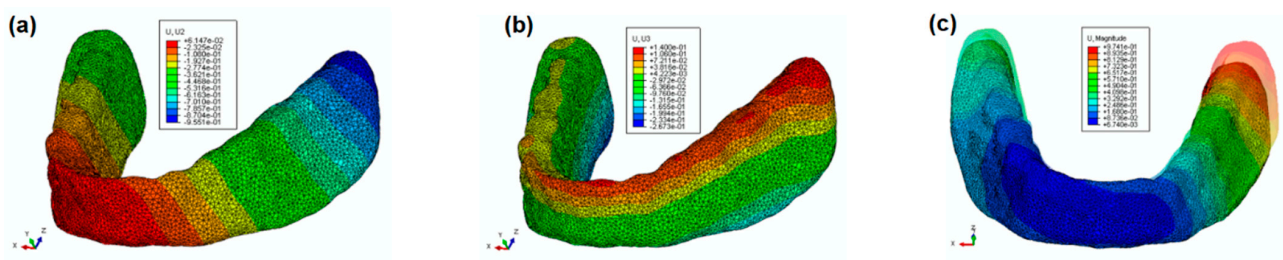


Figure 7. Displacements of the prosthesis along Y (a) and Z axis (b) during canine loading and simplified three-point pin support (c).

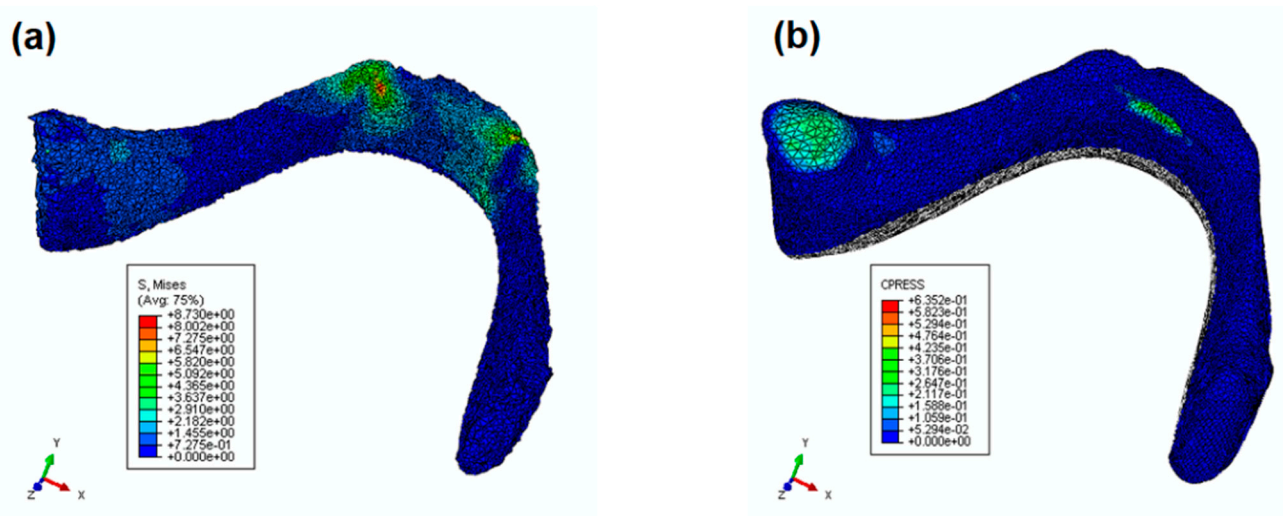


Figure 8. Huber–Mises stress (a) and contact stress distribution (b) on the cortical bone and gingiva, respectively (contour plots for the canine load case and matrix of 3rd level of retention).

Forcing the canine causes a torsional move of the denture in the direction of the working side of the mouth. The plane of the mandibular teeth tilts to one side and results in a gap on the other side. Analogical behavior is observed for molar and incisor bites, but rotations and, thus, occlusion misalignment are the largest for canine excitation. An increase in the bite force causes the progressive degradation of occlusion and more concentrated pressure on the mandible system. In addition, the flexibility of the beam prosthesis joint is only slightly sensitive to the retention level of the applied matrices. This leads to a significant concentration of stress at the anterior (alveolar ridge) and posterior mandible (retromolar pad and linea obliqua) due to biting and chewing (see Figure 8).

The stress distribution under the prosthesis mostly depends on the region loaded onto it. The biting force applied on the foreteeth causes higher contact pressures on the front of the mandible tissues, and their rear zone remains almost unloaded. Such response results from the fact that the force acts along the lines which cross the support location, and only a little swinging on the beam is possible. This indicates good stabilization for the incisor load case, and forces are carried directly by the implants. On the other hand, stress concentration around the implants may cause bone loss (atrophy) in that area. The maximum contact pressure is noted when loads are associated with canines. The critical case for the lower posterior is chewing performed by the molars. The pressure is distributed over a larger area, and hence it reaches lower stress values. Instead, the stress distribution is still nonuniform, and the existence of a mismatch between the prosthesis and mandible can be seen (Figure 9). The maximum stress occurs near the retromolar pad. This region has a significantly different bone structure and higher density [31]; thus, in order to avoid its atrophy, it is vital to ensure that the prosthesis has been well fitted.

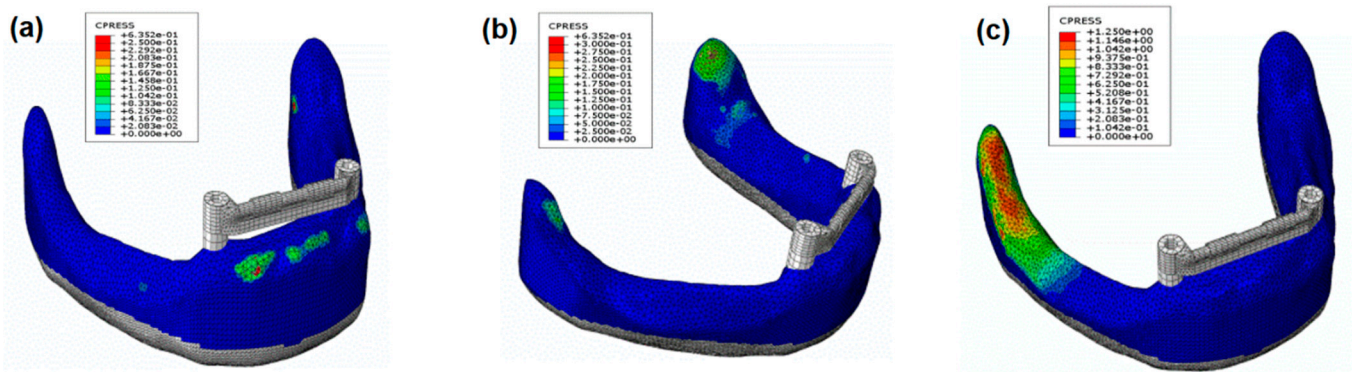


Figure 9. Contact stress distribution over gingiva after the application of the matrices of 2.5 MPa Young’s modulus and for three load cases: biting force on (a) incisor, (b) canine, and (c) molar.

Figure 10 and Table 2 shows horizontal forces, which are carried from the prosthesis to the mandible. For the canine and molar load cases, these forces have the same order of values in both directions (coronal and sagittal), but for the load on the incisor, these forces are different in terms of directions and values.

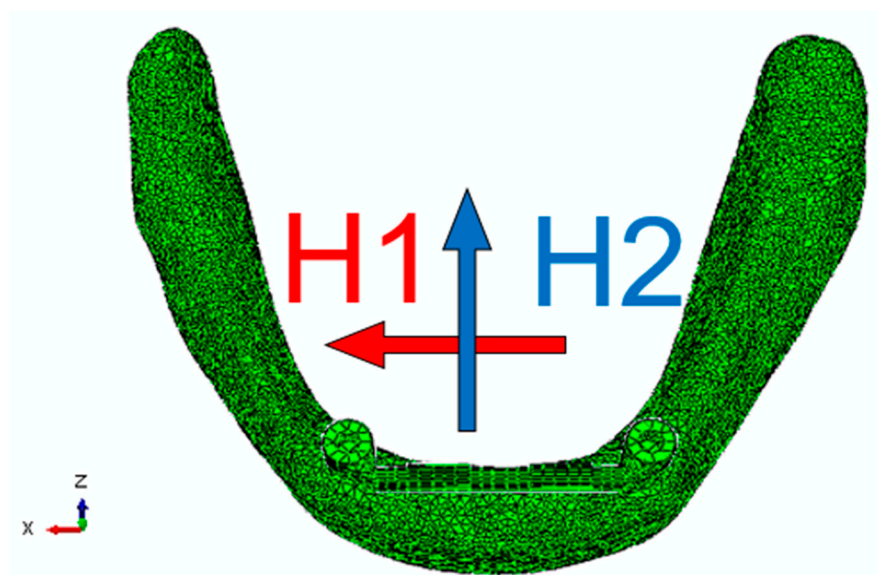


Figure 10. Horizontal forces carried from the prosthesis to the implant system and the dental bar.

Table 2. The values of horizontal forces carried from the prosthesis to the implant system and the dental bar.

Horizontal Force	Canine	Incisor	Molar
H ₁ X axis [N]	+0.095	−0.037	−0.071
H ₂ Z axis [N]	−0.079	+0.111	−0.097

The evaluation of the prosthetic system is performed for typical types of matrices with a few different characteristic retention levels. The most commonly used matrices have Young’s modulus in the range of 2.3–2.8 GPa. The matrix with stiffness equal to 2.5 GPa has a medium retention level, ensuring the average mounting force. Additionally, two extreme matrices with stiffness out of that range are chosen to indicate their effects on how the prosthesis works. The variation of matrix retentions shows no significant

influence, which was expected in simulations. No correlation between retention levels and prosthesis stability was found. The performed analysis shows an insignificant role of matrices in carrying loading from the prosthesis, its movement, and, finally, its stress distribution on the gingiva. Following the use of a stiffer POM-3 matrix, the extreme changes of measurements were small, i.e., the increment of stress = -0.0163 MPa, and the increment of displacements = $+0.0082$ mm (see Figures 11 and 12). These results confirm that prosthesis load bearing and support are independent of the types of POM material. However, it is worth mentioning that the thickness of the matrices is very low, and loads are applied vertically without involving the rotations caused by chewing. The inclusion of exclusive normal biting forces results in the maximum magnitude of a horizontal force per mandible equal to $H_{max} = 0.124$ N, which is less than 1% of the applied load for the canine. The relative changes of the contact area between the mandible and prosthesis caused by different POM properties are presented in Figure 11. The pressure zone is the biggest for POM-1 with Young's modulus of 1.5 GPa and reduced by 5.0% and 7.8% for POM-2 ($E = 2.5$ GPa) and POM-3 ($E = 3.5$ GPa), respectively. Such minor differences between areas of contacting surfaces do not influence the stress field of soft tissues.

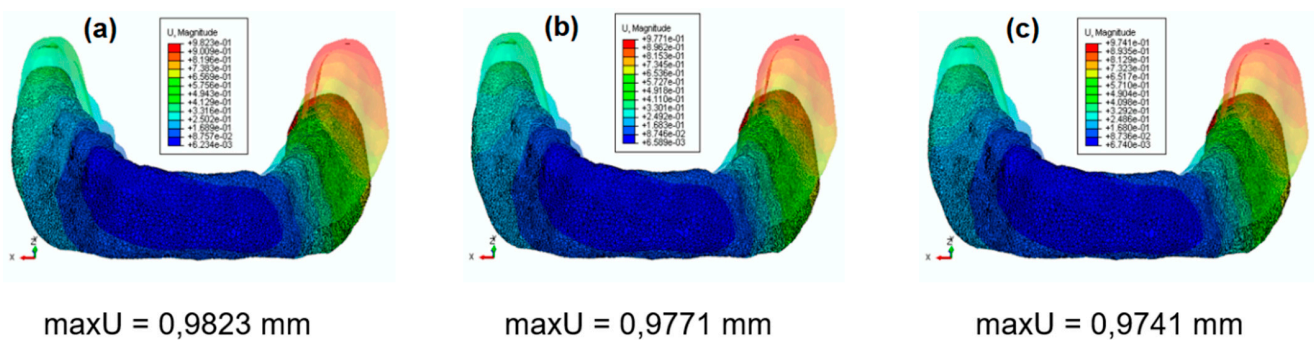


Figure 11. Comparison of the prosthesis movements during canine bite and application of three types of matrices: (a) POM-1, (b) POM-2, and (c) POM-3.

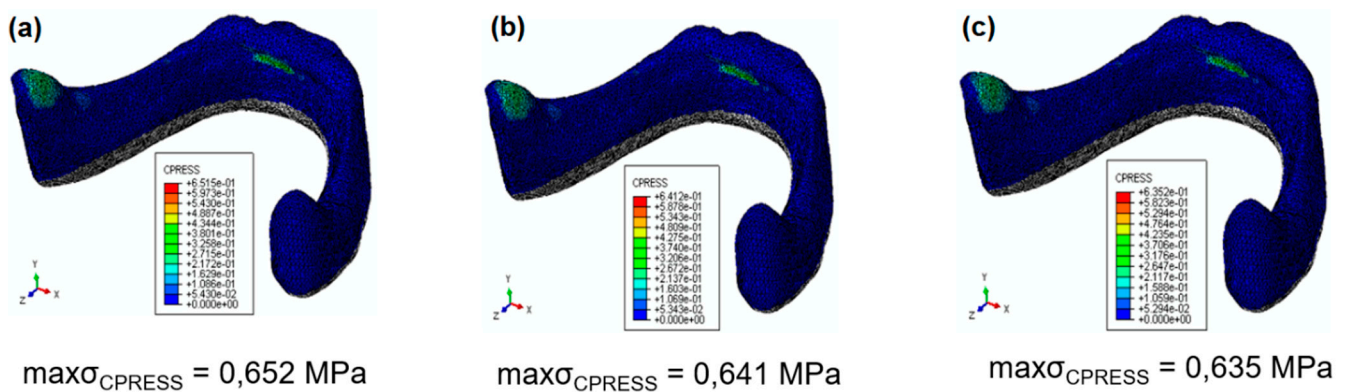


Figure 12. Comparison of the influences of applying POM matrices with three different retention levels on stress distribution results for canine load case and (a) POM-1, (b) POM-2, and (c) POM-3.

Implantoprotheses owe their good retention to friction forces between the matrix and the patrix. Dentures with stiff retention (metal-to-metal friction) are less defective and can be activated periodically. In order to avoid premature retention loss, it is recommended to make the precision attachment of the bars of metal alloys harder than gold alloys [32]. Still, if the abrasion of a metal surface of the bar occurs resulting from the contact with a metal matrix, a replacement of the matrix with a polymer one of lower flexibility is recommended [33]. One of the advantages of polymer matrices is that they are deformable under strain due to their flexible structure. This allows the limited transfer of forces directed

towards prosthodontic area tissues, minimizing axial overload [34]. However, excessive ability to deform under strain may make the denture support in other locations when more significant strain is applied. The force with which the matrix is retained is of less considerable importance, as a change in its stiffness does not affect the value of contact pressures between the denture and its bearing area, which was confirmed in the studies.

Many authors emphasize a significant loss in overdentures retention due to matrices' wear and the need for their replacement [35]. However, the studies by Ortegon et al. (2009) show that in many precision systems, an initial drop in overdenture retention is followed by its stabilization [36]. Bayer's assessment of polymer matrices retention is favorable, though he also noted a decline in their retention from 90% initially to 80% after 6 months of wearing. However, in his in vivo studies, Van Kampen did not notice a decreased retention after three months of wearing overdentures, irrespective of a precision attachment applied (bars, ball attachments, magnets) [37]. Sabavi et al. (2013) extensively covered the issue of mandibular implant prosthesis retention [38]. His studies concerned various bar attachments with single matrices as well as distal cantilever bars and three matrices. Metal and polymer matrices were used, and vertical and anterior–posterior retention was studied. The highest retention was observed for a Dolder bar with distal cantilever bars and three metal matrices; however, a decreased retention was noted in all types of attachments. This research proved that the level of implant prosthesis retention depended on the number, type, and distribution of matrices. Doukas et al. (2008) [39] noticed that retention loss is also related to the location of implants. The greater the distance between implants, the smaller the retention loss with yellow or red matrices.

4. Conclusions

1. In the anterior zone, the applied load produces a slight contact pressure between the denture and the prosthodontic area.
2. In the lateral zone, the applied load produces the largest contact pressure between the denture and the prosthodontic area on the working side around the retromolar pad.
3. This study proved that the most unfavorable forces are those applied to a canine.
4. A change in polypropylene matrix stiffness does not affect the obtained contact pressure field.

Author Contributions: Conceptualization, M.I.-H.; methodology, M.I.-H., T.G., K.S., L.F., M.L.-K.; software, P.B. and K.P.; validation, M.I.-H. and P.B.; formal analysis, A.A.P., T.G., K.S., L.F.; investigation, M.I.-H.; T.G., K.S. and L.F.; resources, M.I.-H., A.A.P. and K.P.; data curation, M.L.-K.; writing—original draft preparation, M.I.-H., T.G., K.S. and L.F.; writing—review and editing, A.A.P.; visualization, K.S. and L.F.; supervision, B.D.-B.; project administration, B.D.-B.; funding acquisition, B.D.-B. and A.A.P. All authors have read and agreed to the published version of the manuscript.

Funding: This research received no external funding.

Institutional Review Board Statement: Not applicable.

Informed Consent Statement: Not applicable.

Data Availability Statement: Not applicable.

Conflicts of Interest: The authors declare no conflict of interest.

References

1. Schierano, G.; Manzella, C.; Menicucci, G.; Parrotta, A.; Zanetti, E.M.; Audenino, A.L. *In vitro* standardization of two different removal devices in cemented implant prosthesis. *Clin. Oral Implants Res.* **2015**, *27*, 1492–1499. [[CrossRef](#)] [[PubMed](#)]
2. Lugas, A.T.; Terzini, M.; Zanetti, E.M.; Schierano, G.; Manzella, C.; Baldi, D.; Bignardi, C.; Audenino, A.L. *In vitro* impact testing to simulate implant-supported prosthesis retrievability in clinical practice: Influence of cement and abutment geometry. *Materials* **2020**, *13*, 1749. [[CrossRef](#)]
3. El-Anwar, M.I.; El-Taftazany, E.A.; Hamed, H.A.; ElHay, M.A.A. Influence of number of implants and attachment type on stress distribution in mandibular implant-retained overdentures: Finite element analysis. *Open Access Maced. J. Med. Sci.* **2017**, *5*, 244–249. [[CrossRef](#)] [[PubMed](#)]

4. Matthys, C.; Vervaeke, S.; Besseler, J.; Doornewaard, R.; Dierens, M.; De Bruyn, H. Five years follow-up of mandibular 2-implant overdentures on locator or ball abutments: Implant results, patient-related outcome, and prosthetic aftercare. *Clin. Implant Dent. Relat. Res.* **2019**, *21*, 835–844. [[CrossRef](#)]
5. Khurana, N.; Rodrigues, S.; Shenoy, S.; Saldanha, S.; Pai, U.; Shetty, T.; Mahesh, M.; Hegde, P. A comparative evaluation of stress distribution with two attachment systems of varying heights in a mandibular implant-supported overdenture: A three-dimensional finite element analysis. *J. Prosthodont.* **2019**, *28*, 795–805. [[CrossRef](#)] [[PubMed](#)]
6. Keshk, A.M.; Alqutaibi, A.Y.; Algabri, R.S.; Swedan, M.S.; Kaddah, A. Prosthodontic maintenance and peri-implant tissue conditions for telescopic attachment-retained mandibular implant overdenture: Systematic review and meta-analysis of randomized clinical trials. *Eur. J. Dent.* **2017**, *11*, 559–568. [[CrossRef](#)]
7. Preti, G.; Martinasso, G.; Peirone, B.; Navone, R.; Manzella, C.; Muzio, G.; Russo, C.; Canuto, R.A.; Schierano, G. Cytokines and growth factors involved in the osseointegration of oral titanium implants positioned using piezoelectric bone surgery versus a drill technique: A pilot study in Minipigs. *J. Periodontol.* **2007**, *78*, 716–722. [[CrossRef](#)]
8. Redžepagić-Vražalica, L.; Mešić, E.; Pervan, N.; Hadžiabdić, V.; Delić, M.; Glušac, M. Impact of implant design and bone properties on the primary stability of orthodontic mini-implants. *Appl. Sci.* **2021**, *11*, 1183. [[CrossRef](#)]
9. Chen, J.; Suenaga, H.; Hogg, M.; Li, W.; Swain, M.; Li, Q. Determination of oral mucosal Poisson's ratio and coefficient of friction from in-vivo contact pressure measurements. *Comput. Methods Biomech. Biomed. Eng.* **2016**, *19*, 357–365. [[CrossRef](#)]
10. Misch, C.E. *Contemporary Implant Dentistry*; International Congress of Oral Implantologists: St. Louis, MO, USA; Mosby, Norway, 1999.
11. Łodygowski, T.; Wierszycki, M.; Szajek, K.; Hędzielek, W.; Zagalak, R. Tooth-implant life cycle design. In *Computer Methods in Mechanics*; Kuczma, M., Wilmanski, K., Eds.; Advanced structured materials; Springer: Berlin/Heidelberg, Germany, 2010; Volume 1.
12. Assuncao, W.G.; Tabata, L.F.; Barao, V.A.R.; Rocha, E.P. Comparison of stress distribution between complete denture and implant-retained overdenture-2D FEA. *J. Oral Rehabil.* **2008**, *35*, 766–774. [[CrossRef](#)]
13. Holmes, P.B.; Wolf, B.J.; Zhou, J. A CBCT atlas of buccal cortical bone thickness in interradicular spaces. *Angle Orthod.* **2015**, *85*, 911–919. [[CrossRef](#)] [[PubMed](#)]
14. *Abaqus Analysis User's Guide*, p. 29.6 Shell Elements; Dassault Systèmes Simulia Corp: Providence, RI, USA, 2015.
15. *Abaqus Analysis User's Guide*, p. 28.1 General-Purpose Continuum Elements; Dassault Systèmes Simulia Corp: Providence, RI, USA, 2015.
16. *Getting Started with Abaqus: Interactive Edition*, p. 4.1 Element formulation and integration; Dassault Systèmes Simulia Corp: Providence, RI, USA, 2014.
17. *Abaqus Theory Guide*, p. 3.2.4 Solid Isoparametric Quadrilaterals and Hexahedra; Dassault Systèmes Simulia Corp: Providence, RI, USA, 2016.
18. *Abaqus Theory Guide*, p. 3.6.5 Finite-Strain Shell Element Formulation; Dassault Systèmes Simulia Corp: Providence, RI, USA, 2016.
19. Fernandez, M.A.; Subramanian, N.; Nawrocki, M.; Nawrocki, A.; Craighead, J.; Clark, A.; O'Neill, E.; Esquivel-Upshaw, J. Finite element analysis (FEA) of palatal coverage on implant retained maxillary overdentures. *Appl. Sci.* **2020**, *10*, 6635. [[CrossRef](#)]
20. *Abaqus Analysis User's Guide*, p. 35.4 Embedded Elements; Dassault Systèmes Simulia Corp: Providence, RI, USA, 2015.
21. *Abaqus Analysis User's Guide*, p. 37.1.2 Contact Pressure-Overclosure Relationships; Dassault Systèmes Simulia Corp: Providence, RI, USA, 2015.
22. *Abaqus Analysis User's Guide*, p. 37.1.5 Frictional Behavior; Dassault Systèmes Simulia Corp: Providence, RI, USA, 2015.
23. Bonnet, A.S.; Postaire, M.; Lipinski, P. Biomechanical study of mandible bone supporting a four-implant retained bridge: Finite element analysis of the influence of bone anisotropy and foodstuff position. *Med. Eng. Phys.* **2009**, *32*, 806–815. [[CrossRef](#)] [[PubMed](#)]
24. Pilarska, A.; Bula, K.; Myszka, K.; Rozmanowski, T.; Szwarc-Rzepka, K.; Pilarski, K.; Chrzanowski, Ł.; Czaczyk, K.; Jesionowski, T. Functional polypropylene composites filled with ultra-fine magnesium hydroxide. *Open Chem.* **2015**, *13*, 161–171. [[CrossRef](#)]
25. Pilarska, A.; Pauksza, D.; Bula, K.; Mazur, M.; Jesionowski, T. Physico-chemical and usable properties of magnesium hydroxide obtained by conversion of various precursors with ammonium hydroxide. *Chem. Ind.* **2012**, *91*, 1400–1406.
26. *Australian Stainless Steel Development Associatic Technical Info*; Dassault Systèmes Simulia Corp: Providence, RI, USA, 2020.
27. Chen, J.; Ahmad, R.; Li, W.; Swain, M.; Li, Q. Biomechanics of oral mucosa. *J. R. Soc. Interface* **2015**, *12*, 20150325. [[CrossRef](#)]
28. Meniccuci, G.; Lorenzetti, M.; Pera, P.; Preti, G. Mandibular implant-retained overdenture: Finite element analysis of anchorage systems. *Int. J. Oral Maxillofac. Implants* **1998**, *13*, 369–376.
29. Hussein, M.O. Stress-strain distribution at bone-implant interface of two splinted overdenture systems using 3D finite element analysis. *J. Adv. Prosthodont.* **2013**, *5*, 333–340. [[CrossRef](#)]
30. Warin, P.; Rungsiyakull, P.; Rungsiyakull, C.; Khongkhunthian, P. Effects of different numbers of mini-dental implants on alveolar ridge strain distribution under mandibular implant-retained overdentures. *J. Prosthodont. Res.* **2018**, *62*, 35–43. [[CrossRef](#)]
31. Čatović, A.; Bergman, V.; Čatić, A.; Seifert, D.; Poljak-Guberina, R. Influence of sex, age and presence of functional units on optical density and bone height of the mandible in the elderly. *Acta Stomatol. Croat.* **2002**, *36*, 327–328.
32. Gajdus, P.; Rzatowski, S.; Idzior-Haufa, M. Overdentures supported by Osteopant implants in difficult types of prosthetic area. *Prosthodontics* **2013**, *63*, 119–126. [[CrossRef](#)]
33. Choy, E.; Reimer, D. Laboratory processing of housing-retained attachments for implant supported overdentures. *J. Prosthet. Dent.* **2001**, *85*, 516–519. [[CrossRef](#)]

34. Zmudzki, J.; Chladek, W. Elastic silicone matrices as a tool for load relief in overdenture implants. *Acta Bioeng. Biomech.* **2008**, *10*, 7–14.
35. Uludag, B.; Polat, S. Retention characteristics of different attachment systems of mandibular overdentures retained by two or three implants. *Int. J. Oral Maxillofac. Implants* **2012**, *27*, 1509–1513.
36. Ortegón, S.M.; Thompson, G.A.; Agar, J.R.; Taylor, T.D.; Perdakis, D. Retention forces of spherical attachments as a function of implant and matrix angulation in mandibular overdentures: An in vitro study. *J. Prosthet. Dent.* **2009**, *101*, 231–238. [[CrossRef](#)]
37. van Kampen, F.; Cune, M.; van der Bilt, A.; Bosman, F. Retention and postinsertion maintenance of bar-clip, ball and magnet attachments in mandibular implant overdenture treatment: An in vivo comparison after 3 months of function. *Clin. Oral Implants Res.* **2003**, *12*, 720–726. [[CrossRef](#)] [[PubMed](#)]
38. Savabi, O.; Nejatidanesh, F.; Yordshahian, F. Retention of implant-supported overdenture with bar/clip and stud attachment designs. *J. Oral Implantol.* **2013**, *39*, 140–147. [[PubMed](#)]
39. Doukas, D.; Michelinakis, G.; Smith, P.W.; Barclay, C.W. The influence of interimplant distance and attachment type on the retention characteristics of mandibular overdentures on 2 implants: 6-month fatigue retention values. *Int. J. Prosthodont.* **2008**, *21*, 152–154.